8th U. S. National Combustion Meeting
Organized by the Western States Section of the Combustion Institute
and hosted by the University of Utah
May 19-22, 2013

A Study of High-Pressure CO_2 Recycling using Pinewood Char Gasification

Indraneel Sircar *Anup Sane* *Jay P Gore*

Maurice J. Zucrow Laboratories, School of Mechanical Engineering, Purdue University, 500 Allison Road, Chaffee Hall, West Lafayette, IN 47907-2014

Measurements of the gasification reaction rates at high-pressures for a low-ash pinewood char with pure CO_2 are presented. A fixed-bed reactor operated at 1140-1260 K and 1-10 atm was utilized to study the reaction rates. Product gas sampling and gas chromatography measurements enabled tracking of the gasification progress and mass loss data. The mass loss data are interpreted using the volumetric and non-reactive core models. Activation energy, collision frequency and reaction order are reported for each model. The experimental data show very high sensitivity to temperature. The data also show an increase of the apparent gasification rates with higher CO_2 pressures. Comparison of computed char conversion profiles and experimental data are discussed in the context of mass transport and char structure effects on the gasification rates. The findings from this study have applications to gasification modeling and design of large-scale gasification systems.

Keywords: Biomass, Gasification, Renewable Energy, Kinetics, Char

1. Introduction

Gasification is an important thermo-chemical conversion process in the production of liquid fuels, chemicals and power from biomass or coal [1-3]. Gasification is the partial oxidation of a solid carbonaceous feedstock to a syngas (mixture of carbon monoxide (CO) and hydrogen (H_2)) in presence of oxidizing agents, mainly water vapor (H_2O) and carbon dioxide (CO_2). Gasification reactions are endothermic in nature. In industrial gasifiers operating on auto-thermal cycle, combustion of a small part of the input feedstock with O_2 is used for establishing a high temperature environment to support gasification. Gasification is a two-step process that involves two global reactions: 1) the carbonaceous feedstock is pyrolyzed to release volatile organic matter, and 2) the resulting char is oxidized by H_2O and CO_2 to produce CO and H_2. The gasification reactions are slow and energy intensive making them the process rate-determining step and the topic of many investigations.

Gasification by CO_2 is relevant to operation of auto-thermal gasifiers and oxy-coal combustors operating with CO_2 recycling. It is also relevant to the chemical process and metal industries where reactions between carbonaceous feedstock and oxidizers are conducted for chemical synthesis or metal enriching. Biomass gasification by CO_2 is an active research topic because it is a potential renewable energy technology that can be combined with chemical looping technologies to develop clean power devices [4]. In the next section, a brief review of recent small-scale CO_2 biomass gasification investigations is presented to establish the scope for this work. The reader is directed to review articles by Balat et al. [5] and McKendry [6] for a more comprehensive discussion of past studies of biomass gasification.

The investigation of CO_2 biomass gasification kinetics at atmospheric pressure has been recently conducted by several researchers. Seo et al. [7] studied the CO_2 gasification reaction of pinewood char at 750-900 ^oC in a fixed-bed reactor and demonstrated that mathematical modeling of the gasification reaction using appropriate reaction rate constants can

show good agreement with experimental data. Butterman and Castaldi [8] performed extensive studies of the CO_2 gasification reaction of various biomass at 110-980 ^oC. The experiments were conducted by heating a single batch of feedstock from ambient to 980 ^oC temperature at constant heating rates in contrast to most studies that have been performed in isothermal environments. Their results showed that biomass with high proportion of lignin, such as alfalfa, had lower activation energies in contrast to materials with higher proportion of cellulose such as hard woods. Mani et al. [9] investigated the impact of the reaction temperature and the particle size on the CO_2 gasification behavior of birch and pinewood chars at 750-900 ^oC. Their study showed that the gasification rate is most sensitive to the reaction temperature and reaction rates increased with temperature for small particles. Mitsuoka et al. [10] investigated the impact of ash and alkali metals (calcium and potassium) on the CO_2 gasification rates of a Japanese cypress at 1123-1223 K. Gasification of Ca/K pre-treated cypress char showed significant increases in the reaction rates relative to the un-treated char. Irfan et al. [11] investigated the gasification reaction rates of palm shells in CO_2/O_2 mixtures at temperatures of up to 1000 ^oC. They observed a decrease in the activation energy for the C-CO_2 reaction when O_2 fraction in the reactant gas was increased from 22% to 80%. Lahijani et al. [12] investigated the influence of iron on the gasification rates of oil palm shell chars at 800-1000 ^oC. The reaction rates increased with the addition of the iron catalyst to the char. Umeki et al. [13] investigated the effect of the ash content and ash composition of nine biomass chars on the CO_2 gasification rates at 1023-1123 K. Their study showed that the char reaction rates varied with char conversion due to the changing ash-to-carbon ratio. Aho et al. [14] studied the impact of alkali metals on the CO_2 gasification rates of pinewood char at 805 ^oC. Peak gasification rates for the char increased by factors of 3-4 when the pinewood had been doped with calcium or manganese.

Investigations of high-pressure CO_2 biomass gasification have been scarce in comparison to the number of studies conducted at atmospheric conditions. Several studies of high pressure gasification of coal exist and have been extensively reviewed by Wall et al. [15]. Relatively recent coal-CO_2 gasification experiments at high pressure were conducted by Roberts et al. [16-18]. However, the use of coal gasification data for biomass gasification reaction modeling is difficult due to the inherent physical and chemical differences of the two materials. Therefore, high-pressure gasification biomass gasification experiments similar to previous coal gasification studies are needed. Fermoso et al. [19] studied the gasification of pine at 750-900 ^oC at total pressures of 1 and 10 bar with varying CO_2 partial pressures. Their investigation found the gasification reaction rate to be sensitive to the CO_2 partial pressure and independent of the total pressure. Cetin et al. [20,21] studied the impact of total pressure on the gasification reactivity of a pine char at 1-20 bars and up to 900 ^oC. The char used in their experiments was prepared at conditions similar to the gasification environment. Their investigation found a decrease in the apparent reactivity for chars that were prepared and gasified at high pressures. The decrease in the apparent reactivity at the higher pressures was explained by the development of non-reactive crystalline graphitic lattice structures during the pyrolysis process. High total pressures showed insignificant effects on the mass transport properties in their study. Illerup and Rathmann [22] investigated the CO_2 gasification rates of wheat straw, barley straw, willow and elephant grass at 700 – 900 ^oC at 1 – 20 bar. Their studies indicated that total pressure had insignificant impact on the gasification rates as well. Blackwood and Ingeme [23] conducted one of the earliest high-pressure gasification investigations of a coconut char with CO_2-CO mixtures up to 40 atm. Their studies showed that the gasification reactivity of the coconut char increased significantly with total pressure at initially low pressures. At higher pressures, the reaction rate increased proportionately with total pressure. This observation was explained by the inhibiting effects of the produced CO on the gasification reaction. The effects of pressure on the biomass feedstock and its gasification rates are still inconclusive due to the limited high-pressure investigations and present opportunities for numerous experimental investigations. A summary of gasification studies and the kinetic parameters from the discussed studies is presented in Table 1. The reader is also directed to the work by Butterman and Castaldi [8] for an exhaustive list of gasification studies and kinetic parameters.

This work investigates the gasification of a low-ash pinewood char in presence of CO_2 in a hot rod fixed bed reactor. Hot gases flow over the biomass particles in a top down configuration and transfer heat to the particles to the reaction temperature. The pinewood char used in the gasification experiments are prepared in a single batch to have uniform properties and to enable study of the gasification process only. Results from gasification experiments at isothermal reaction temperatures (1140-1260 K) at high pressures (1 – 10 atm) are reported. Reaction rate constants are calculated from the experimental data using the n^{th}-order volumetric [28,29] and non-reactive core [29] reaction models. The assumptions for the two models are analyzed through comparison with experimental char conversion data. The experimental and numerical reaction rate histories are compared and discussed in the context of the chemical and physical processes that are sensitive to temperature and pressure.

Table 1. A summary of nth-order model kinetic rate constants for different biomass feedstock from prior studies.

Study	Biomass	Temperature [^{o}C]	Particle Size [μm]	Activation Energy, E_a, (kJ/mol)	Pre-exponential Constant, A, (s^{-1}-P^{-n})	n
Volumetric Reaction Model						
Butterman and Castaldi [8]	Pine	110-980	Powdered	141	-	1
Fermoso et al. [19]	Pine	750-900	75-106	184	6.5e8	~0.34*
Seo et al. [7]	Pine	850-1050	250-300	172	5.4e7	-
Bhat et al. [24]	Rice husk	750-900	10	197	-	-
Ollero et al. [25]	Olive residue	800-950	45-150	133	1.68e2	0.43
Cetin et al. [21]	Pine Eucalyptus Bagasse	785-1000	120-180	224-238 233 198	2.15e7 – 4.47e7 1.98e7 3.15e5	0.48 0.39 1
Barrio and Hustad [26]	Birch	750-950	32-45	215	3.1e6	0.38
Tancredi et al. [27]	Eucalyptus	400-1000	~ 200	230-260	-	-
De Groot and Shafizadeh [28]	Douglas fir Cottonwood	700 – 900	42-700	220 196	1.96e9 4.85e8	-
Non-reactive Core Model						
Seo et al. [7]	Pine	750-900	75-106	142	2.3e6	-
Fermoso et al. [19]	Pine	750-900	75-106	185	5.3e9	~0.34*
Bhat et al. [24]	Rice husk	750-900	10	180	-	-

* >1 atm

2. Methods

2.1 Experimental Arrangement

Figure 1 shows a schematic diagram of the reactor arrangement. The reactor is 90 cm tall, has an inner diameter of 2 cm and a wall thickness of 2 mm. Reactant gases enter the reactor from the top and flow downwards. The central 30 cm of the reactor is the heated zone, which houses the bed. The reactor is designed for pressures of up to 13 atm and temperatures of up to 1300 K. The operating conditions of the reactor are remotely monitored and automated. The reactor can reach a temperature of 1300 K from ambient temperature within 20 minutes (average heating rate ≈ 50 K/min). The heat input for the reactions is provided by surrounding electrical radiant heaters. Pressure transducers enable measurements of the reactor pressure during the experiments.

The bed is constructed by welding two layers of stainless steel wire meshes onto which biomass feedstock is dispersed. The bed is supported on a honey-comb that fits tightly within the reactor and holds the bed at a fixed location. The reactant gases flow over the bed and transfer heat to the feedstock. Thermocouples measure the temperature of the reactant gases approximately 2 cm above the bed and maintain the temperature to within 10 K from the set-point. Product gases exit through the bottom spool and are cooled and filtered before gas sample collection. Gas samples are analyzed using a Shimadzu GC-8AIT gas chromatograph (GC) for species composition.

2.2 Char Preparation

Char is prepared by inert heating of a large quantity of the raw pinewood sawdust in the reactor. Table 2 presents the proximate and the ultimate analyses of the raw pinewood sawdust. The reactor, filled with raw pinewood sawdust, is

heated at 3 K/minute to 1100 K at atmospheric pressure with a continuous flow of nitrogen, at rate of 0.30±0.01 g/s. Once the reactor reaches 1100 K, the heaters are turned off and the reactor is allowed to cool. Nitrogen is flowing during the cooling process at 0.15±0.01 g/s to avoid any reaction of the char with atmospheric air. At the end of the cooling cycle, char is removed from the reactor for use in gasification experiments. Energy-dispersive-spectroscopic measurements of the resultant char show greater than 99% fixed carbon content by mass.

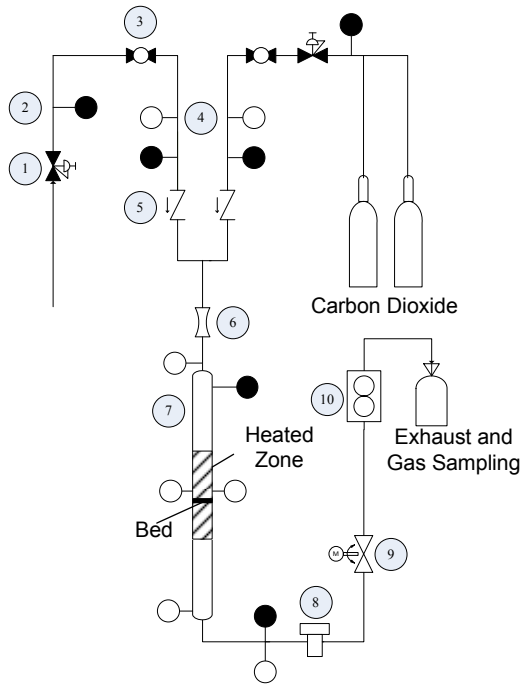

Figure 1: Schematic of fixed bed reactor arrangement. Diagram components: 1. pressure regulator, 2. pressure transducer, 3. on-off valve, 4. thermocouple, 5. check valve, 6. mass-flow controlling orifice, 7. fixed-bed reactor, 8. filter, 9. back-pressure controller, 10. flow-rate meter.

Table 2: Proximate and ultimate analyses for the pinewood sawdust (All values presented in weight %).

Proximate Analysis			
Moisture	Volatile Matter	Fixed Carbon	Ash
7.29	77.92	15.52	<0.01

Ultimate Analysis				
Carbon	Hydrogen	Nitrogen	Oxygen	Sulfur
51.20	6.05	0.16	38.35	<0.005

The char particles are sorted using a vibratory sieve shaker. The char particles were closer to slab-shaped than spherical and the mentioned sizes are the sieve spacing. Most of the char particles are within 1168-3350 µm. All other sized particles are discarded. A 50:50 weight percentage of char particles within 1168-1680 and 1680-3350 µm are used in gasification experiments. The feed to a practical gasifier contains particles of a wide distribution of sizes and shapes. Gasification rates for large particles are critical for the design of industrial-scale gasification arrangements and this study uses char with size and shape distributions that are more representative of feed used by commercial gasifiers.

2.3 Gasification of Pinewood Char with CO_2

A known mass of char is dispersed as a thin layer onto the bed and loaded into the reactor for gasification. Air and moisture in the reactor are removed by flowing N_2 for fifteen minutes before the start of the experiment. The char is heated at an average heating rate of 50 K/minute to the experiment temperature with a continuous N_2 purge. The gasification stage begins once the reactor reaches the experiment temperature and the CO_2 replaces the N_2 flow. Fifteen product gas samples are collected at one-minute interval for the first fifteen minutes of the gasification experiment. Fifteen product gas samples are collected at three-minute separation over the next forty-five minutes of the gasification

experiment. CO_2 is replaced by the N_2 flow and the heaters are turned off at sixty minutes concluding the experiment. CO_2 is removed from the reactor by purging with N_2 and the reactor is left to cool down. The reactor is then disassembled and the residual feedstock is collected and weighed to calculate final mass conversion. The common operating parameters for the experiments are presented in Table 3. Gasification experiments were conducted at 1140, 1160, 1200, 1240 and 1260 K at 1, 5 and 10 atm. A total of 15 pressure-temperature combinations were investigated.

Table 3: Common operating parameters for the pinewood char gasification experiments.

Experimental Parameter	**Units**	**Value**
N_2 flow-rate for heating	g/s	0.25 ± 0.01
CO_2 flow-rate for gasification	g/s	0.25 ± 0.01
Mass of char	g	0.50 ± 0.01
Duration of gasification	min	60

2.5 Analysis of Experimental Data

The global C-CO_2 reaction, shown by Equation (1), is investigated in this study. Measured values of CO concentration in the product gas along with product gas flow-rates are used to quantify the char conversion rates. Based on mass conservation, the production rates for CO and char are related by Equation (2) under the assumptions of negligible accumulation of products and a thin reaction layer.

$$C(\text{char}) + CO_2 \rightarrow 2CO,\ \Delta H = 172.67,\ \text{kJ/gmol-C} \tag{1}$$

$$\dot{\omega}_{co} = Y_{co}\dot{m}_{out} = -2\dot{\omega}_{char}\ {MW_{co}}\big/{MW_{char}} \tag{2}$$

The char conversion, *X*, is determined from the CO composition measurements, and described by Equation (3).

$$X = 1 - {m_{char}}\big/{m_{char,t=0}} = 1 - \frac{\left(m_{char,t=0} - \left({MW_{char}}\big/{2MW_{co}}\right)\int_0^t \dot{\omega}_{co}\,dt\right)}{m_{char,t=0}} \tag{3}$$

The volumetric and non-reactive core n^{th}-order reaction models are used to interpret the experimental data. The volumetric reaction model is presented by Equation (4) and assumes that the reaction is occurring uniformly throughout the volume.

$$X = 1 - \exp(-Kt) \tag{4}$$

The non-reactive core model, described by Equation (5), assumes that the reaction initiates on the external surface of a particle and gradually progresses inwards.

$$X = 1 - (1 - Kt)^3 \tag{5}$$

In both models, the apparent reaction rate constants, *K*, and the chemical reaction rate constants, *k*, are related by the total pressure, shown as Equation (6).

$$K = k({P}/{P_{ref}})^n,\ \text{P}_{\text{ref}} = 1\ \text{atm} \tag{6}$$

Equations (4)-(5) are linearized with respect to time, as shown by Seo et al. [7], to obtain the apparent reaction rate, *K*. A ratio of apparent reaction rates from experiments conducted at one temperature leads to Equation (7) to enable

calculation of the reaction order, assuming that the chemical kinetic rate constant, *k*, is only a function of temperature. The chemical kinetic rates, *k*, are assumed to follow the Arrhenius rate law. Arrhenius plots are used to determine the pre-exponential factor, *A*, and the activation energy, E_a, for each reaction model.

$$K = k(P / P_o)^n \rightarrow \ln(K_2 / K_1) = n \ln(P_2 / P_1), \quad T_2 = T_1 \tag{7}$$

$$k = A \exp(-E_a / (R_u T)) \tag{8}$$

3. Results and Discussion

The temperature histories for the CO_2 gasification experiments are shown in Figure 2. Control of the bed temperature to within ± 10 K was achieved during the gasification experiments, minimizing temperature-sensitive fluctuations of the reaction rates. Oscillations in the temperature history are caused by the action of the PID heater controller. Figure 3 displays the reactor pressure histories during the gasification experiments. The spikes in the pressure trace for the 1 atm experiments are caused by the momentary backpressure developed during the product gas sample collection. These fluctuations occur for less than 10% of the total gasification duration and are expected to have negligible impact on the gasification reaction. The pressures were controlled to within ± 0.2 atm for the high pressure experiments.

Measurements of the CO mole-fractions in the product gas samples by a gas chromatograph are presented in Figure 4. The C-CO_2 reaction is temperature sensitive and the CO production rate is observed to increase with temperature. Figure 4 also shows that the CO production increases with the CO_2 pressure. An increase in the CO production due to an increase in pressure may be explained by a higher CO_2 surface concentration due to enhanced external and internal mass transport of reactant gases. Transport of reactant gases into the particle may increase the number of reactive sites that can participate in the gasification reaction, leading to the larger apparent reaction rates observed. This process is particularly important for biomass feedstock because they contain greater surface area from macropores in comparison to coal.

The exceptions to this observation are the 5 and 10 atm experiments at 1240 and 1260 K. There is little difference in the magnitude of the CO production between the 5 and 10 atm experiments at these temperatures. The diminishing increase in the CO production at higher pressures may be explained by micropore development in the char particle. Micropore development is important to gasification reactions because the majority of the reactive surface area in the intermediate stages of gasification is contained within the micropores. The diminishing effect of total pressure on the CO production rate at high pressures may be explained by the micropore diffusion limits when micropore diffusion is controlled by the Knudsen diffusion process [15,17,30], which is unaffected by pressure.

Alternatively, the diminishing reaction rate with pressure may also be explained by the accumulation of CO at the reactive surface. Higher total pressures may impede the diffusion of gasification products from the particle surface to the bulk stream. The accumulation of CO at the surface will displace CO_2 resulting in lower surface CO_2 concentrations and lower apparent reaction rates. This effect has also been observed and explained in other experimental [18,23] and computational [31,32] gasification studies.

The CO mole-fraction measurements are used to calculate char conversion histories shown in Figure 5. Final char conversions were confirmed by mass measurements of the post-gasification remaining feedstock using a micro-balance scale. The final conversion values increase with a rise in pressure. Complete conversion of the feedstock is achieved within 5 minutes at 1260 K and 10 atm. Figure 5 also shows that an increase in the pressure from 1 atm to 5 atm produces a larger rise in the apparent gasification rate than an increase from 5 atm to 10 atm. For example, the final conversion at 1140 K increases by 39% when pressure is raised from 1 to 5 atm, but only 21% when the pressure is raised from 5 to 10 atm. This supports our earlier discussion of the diminishing impact of pressure on the apparent reaction rate.

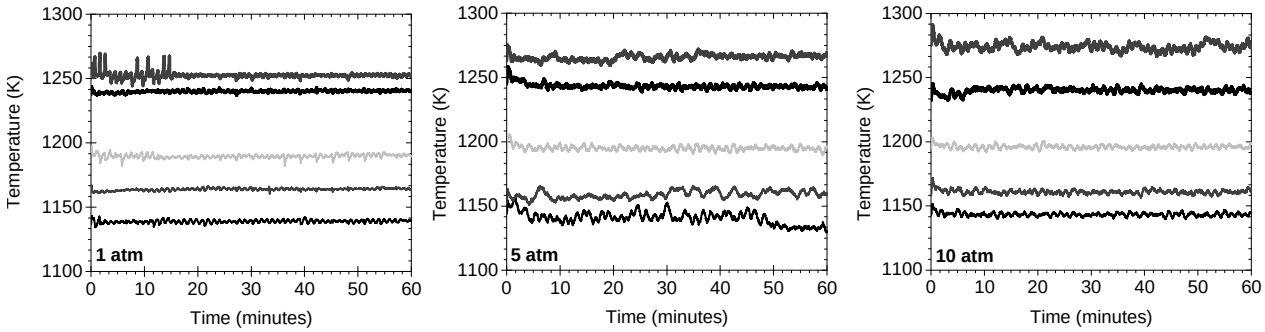

Figure 2: Bed temperature history during the gasification experiments. Temperatures shown in ascending order: 1140 K, 1160 K, 1200 K, 1240 K, and 1260 K.

Table 4 presents the chemical kinetic rates and the reaction order for the experimental data at each temperature. The chemical kinetic rates increase with the reaction temperature. The order of the reaction with respect to the CO_2 pressure for both models is approximately 1. The order for the volumetric model increases from ~ 1 under 1200 K to ~ 1.27 at 1200 K and greater. The order for the non-reactive core model increases monotonously with the reaction temperature. This trend shows that mass transport becomes more important when the reaction temperature increases because the apparent reaction rate is transitioning from kinetic to diffusion control.

The pre-exponential factor, A, and the activation energy, E_a, were calculated from Arrhenius plots. Values for A and E_a for the gasification reaction are presented in Table 5. The chemical kinetic constants from this study agree with values from the literature presented in Table 1. The reaction order may be slightly higher than most reported in the literature, but could result from the larger sized particles used in this study. The diffusion boundary will be thicker for larger sized particles.

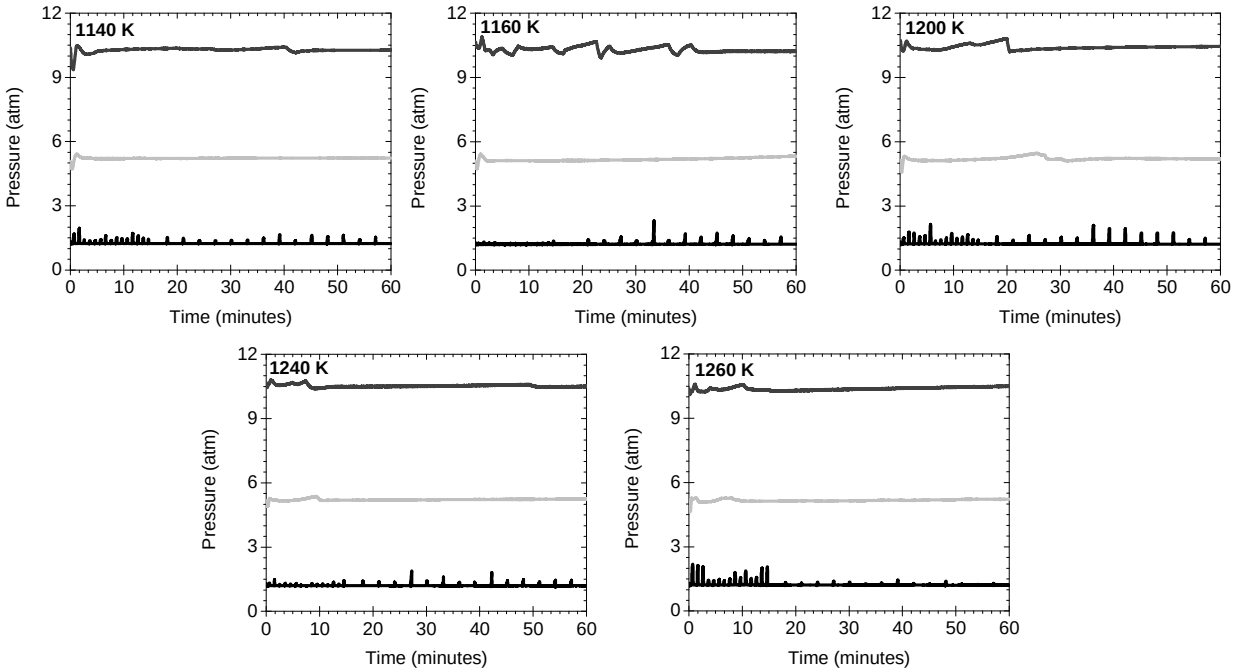

Figure 3: Pressure history for the gasification experiments (black: 1 atm, light gray: 5 atm, dark gray: 10 atm).

Table 4: Experimental chemical reaction rates and reaction order for the gasification experiments.

Reaction Model	Variable	Reaction Temperature				
		1140 K	1160 K	1200 K	1240 K	1260 K
Volumetric	$k \pm \sigma_k$ (s^{-1})	9.38e-5 ± 9.97e-6	1.90e-4 ± 1.17e-5	2.54e-4 ± 3.34e-5	7.19e-4 ± 4.21e-5	8.84e-4 ± 5.03e-5
	n	0.97	0.94	1.28	1.31	1.21
Non-reactive Core	$k \pm \sigma_k$ (s^{-1})	3.10e-5 ± 2.01e-6	5.70e-5 ± 8.61e-6	7.33e-5 ± 1.73e-5	1.71e-4 ± 8.41e-6	1.93e-4 ± 2.69e-5
	n	0.84	0.85	1.09	1.20	1.23

Table 5: Activation energy, E_a, pre-exponential factor, A, and average reaction order, n.

Reaction Model	Activation Energy, E_a (kJ/mol)	Pre-exponential Factor, A (s^{-1})	n	Coefficient of Determination (R^2)
Volumetric	213	5.66e5	1.1	0.963
Non-Reactive Core	174	3.15e3	1.0	0.936

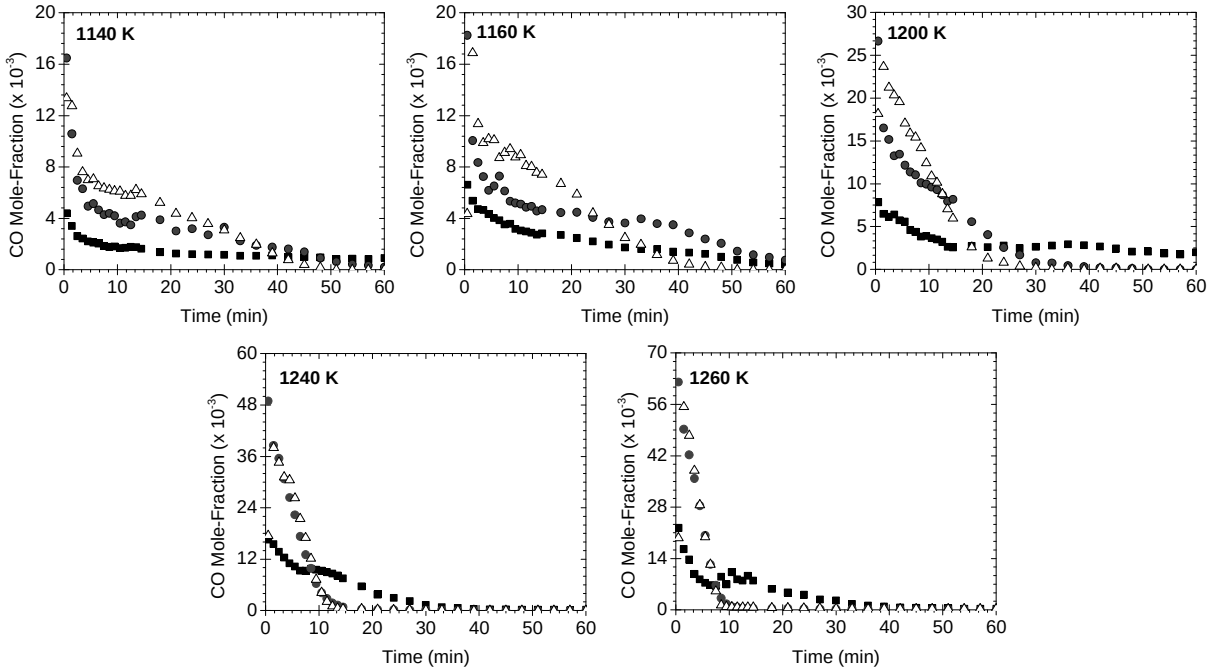

Figure 4: CO mole-fraction in product gas samples measured by gas chromatograph (■: 1 atm, ●: 5 atm, Δ: 10 atm). Uncertainty bars are not shown to avoid clutter. Uncertainty with 95% confidence = ± 6%.

Char conversion histories were computed by the volumetric and the non-reactive core models and are shown in Figures 6 and 7 respectively. The models show reasonable agreement with the experimental data, but neither matches the experimental data perfectly. The change in the apparent reaction rates due to pressure is captured by the computations. The agreement between the experimental and computed conversion histories support the hypothesis that total pressure controls the mass transport processes of the reactant gas, but has insignificant impact on the chemical reaction.

The volumetric model shows better agreement with the experimental data at the atmospheric conditions whereas the non-reactive core model shows better agreement with high pressure data. The volumetric model does not consider the effects of mass diffusion due to the assumption of homogeneously mixed reactants. This assumption leads to higher than

observed reaction rates at the initial and intermediate stages of gasification. On the other hand, the non-reactive core model assumes that the reaction is limited to the surface. The assumption of the reaction being limited to the surface is inaccurate, but considers internal mass transfer resistance. This may be the reason that the non-reactive core model produces better agreement with the experimental data at the initial stages. Neither model produces a perfect agreement with the experimental data since the discussed physical processes are not mutually exclusive. Furthermore, neither model incorporates the effects of a changing char structure on the apparent reactivity. The char structure evolution is better represented by models like the random pore model [33] and will be a topic of future study.

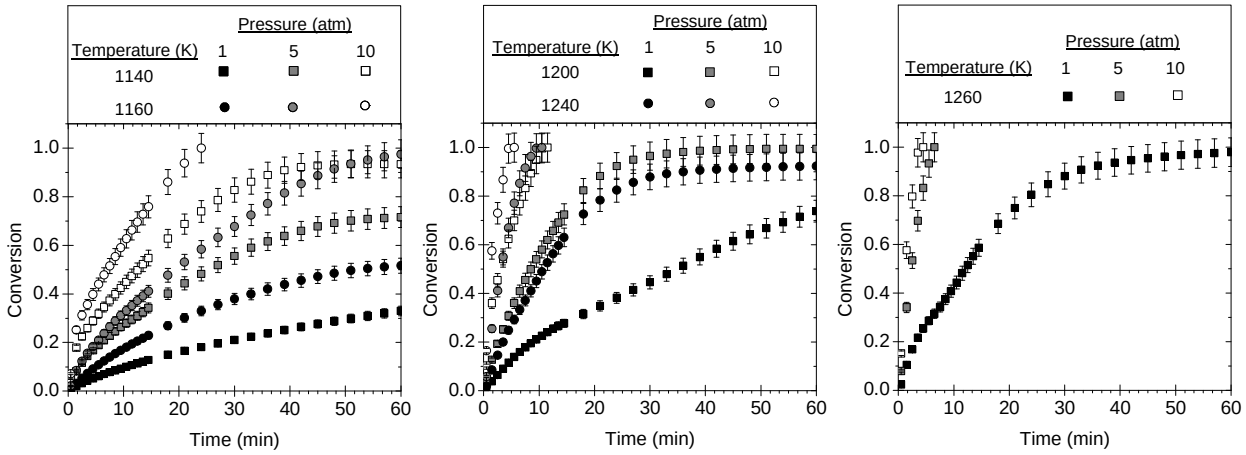

Figure 5: Char conversion histories calculated using the control-volume approach. Error bars represent 95% confidence intervals.

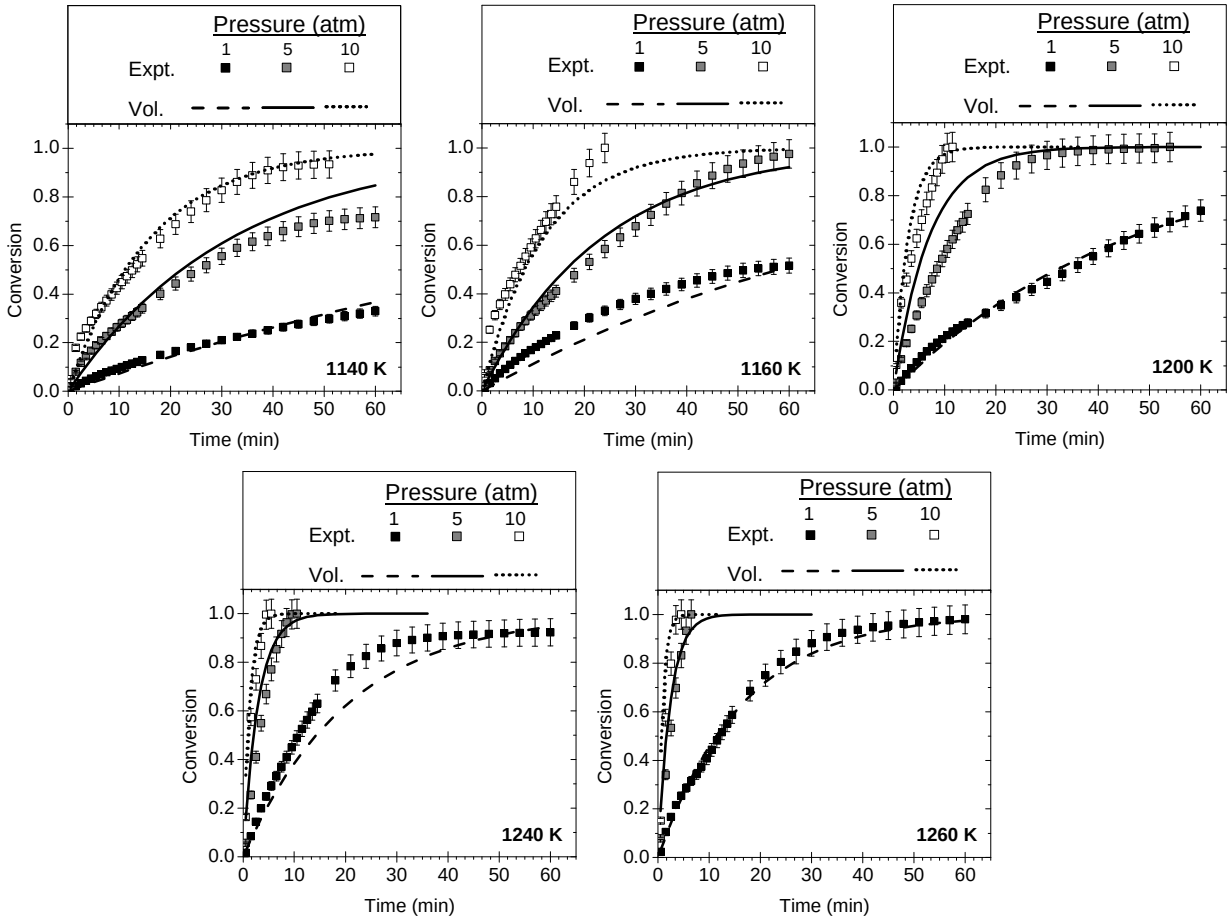

Figure 6. Experimental conversion histories and computed conversion histories with the volumetric model.

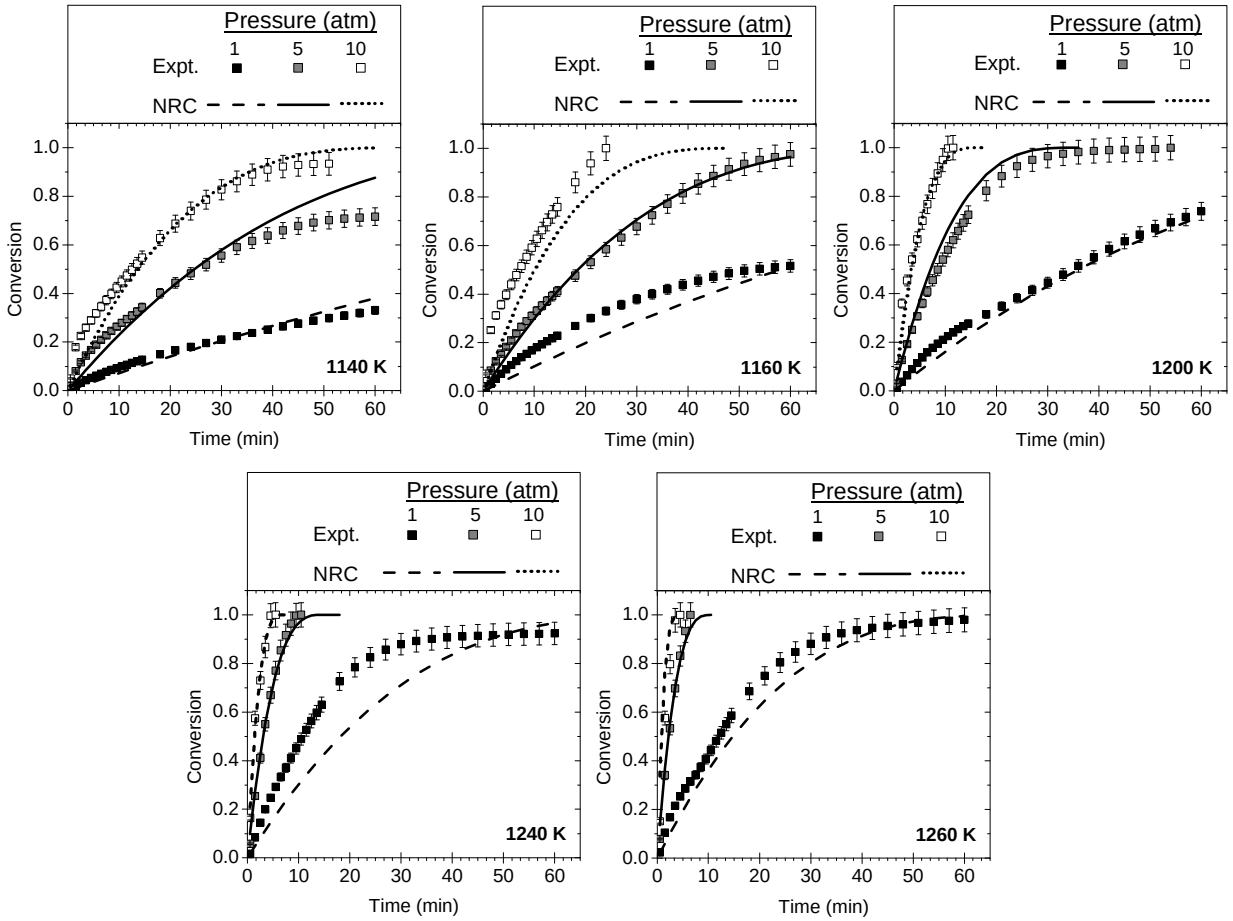

Figure 7: Experimental conversion histories and computed conversion histories with the non-reactive core model.

4. Conclusions

Gasification of a low-ash pinewood char with CO_2 was investigated at 1-10 atm and 1140-1260 K in a fixed-bed gasifier. Measurements of char conversion and CO production rates were presented for the gasification duration. Chemical kinetic constants and reaction order for the char-CO_2 gasification reaction were reported for the volumetric and non-reactive core models. Computed char conversion histories from the mathematical models were compared with the experimental data. The conclusions from this study are summarized as:

(a) The char-CO_2 reaction is temperature sensitive and the reaction rate increases with temperature. The total conversion increased from 33% to 98% when the temperature was raised from 1140 K to 1260 K at 1 atm.

(b) The char-CO_2 apparent reaction rate increases with the CO_2 pressure up to 10 atm. The impact of pressure on the apparent gasification rate diminishes at higher pressures; i.e. at 1140 K, the final conversion increases by 39% and 21% when the pressure is raised from 1 atm – 5 atm and from 5 atm – 10 atm respectively.

(c) The expressions for the volumetric and non-reactive core reaction rate constants for the pinewood char-CO_2 reaction investigated are:

$$k_v = (5.66e5)\left(\frac{P}{P_0}\right)^{1.1} \exp\left(\frac{-213\ \text{kJ-mol}^{-1}}{R_u T}\right) \text{s}^{-1}$$

$$k_{nrc} = (3.15e3)\left(\frac{P}{P_0}\right) \exp\left(\frac{-174\ \text{kJ-mol}^{-1}}{R_u T}\right) \text{s}^{-1}$$

(d) The order of the reaction with respect to the CO_2 pressure is approximately 1 for both reaction models and can be attributed to the larger sized particles utilized in this study in comparison to other works.

(e) The n^{th}-order rate models show good agreement with the experimental data. The non-reactive core model shows better agreement with the high-pressure reaction data than the volumetric model.

(f) Pressure has a significant impact on the mass transport processes of CO_2 to the particle and thereby affects the apparent gasification reactivity. There is little evidence to show that pressure has significant impact on the chemical reactivity of the biomass char.

This study demonstrates that apparent gasification rates at low temperatures can be significantly increased by raising the pressure. Future studies will elaborate on the current work by investigating the char structure development with conversion at various pressure-temperature conditions and describe the dominant transport processes involved at the different stages of gasification. The findings from this study have applications for modeling and design of energy efficient industrial gasification systems.

Notation

$\dot{\omega}$	= production rate, *g/s*	E_a	= activation energy, *kJ/mol*
Y	= mass fraction	R_u	= ideal gas constant, *8.314 kJ/kmol-K*
$\dot{m}$	= rate of mass flow, *kg/s*	T	= temperature, *K*
MW	= molecular weight, *g/mol*	P	= pressure, *atm*
X	= conversion fraction	n	= reaction order
m	= mass, *kg*	v	= volumetric reaction model
t	= time, *s*	nrc	= non-reactive core model
k	= reaction rate constant, s^{-1}	A	= pre-exponential constant, s^{-1}
K	= apparent reaction rate, s^{-1}	k	= chemical (intrinsic) reaction rate, s^{-1}

Acknowledgements

We thank ALS-Columbia for providing the material analyses for the pinewood feedstock. We acknowledge Rob McGuire's assistance in design and fabrication of the experimental arrangement. We appreciate the contributions of Weichao Wang and Yicheng Yang in obtaining the experimental data.

References

[1] Agrawal R, Singh NR, Ribeiro FH, Delgass WN. Sustainable fuel for the transportation sector. Proceedings of the National Academy of Sciences. 2007;104(12):4828-33.

[2] Bridgwater AV. The technical and economic feasibility of biomass gasification for power generation. Fuel. 1995;74(5):631-53.

[3] Hotchkiss R. Coal gasification technologies. Proceedings of the Institution of Mechanical Engineers Part a-Journal of Power and Energy. 2003;217(A1):27-33.

[4] Moghtaderi B. Review of the Recent Chemical Looping Process Developments for Novel Energy and Fuel Applications. Energy & Fuels. 2012/01/19 2011;26(1):15-40.

[5] Balat M, Balat M, Kırtay E, Balat H. Main routes for the thermo-conversion of biomass into fuels and chemicals. Part 2: Gasification systems. Energy Conversion and Management. 2009;50(12):3158-68.

[6] McKendry P. Energy production from biomass (part 3): gasification technologies. Bioresource Technology. 2002;83(1):55-63.

[7] Seo DK, Lee SK, Kang MW, Hwang J, Yu T-U. Gasification reactivity of biomass chars with CO_2. Biomass and Bioenergy. 2010;34(12):1946-53.

[8] Butterman HC, Castaldi MJ. Experimental and Kinetic Investigation of CO_2 and H_2O/N_2 Gasification of Biomass Fuels. Synthetic Liquids Production and Refining. Vol 1084: American Chemical Society; 2011:27-73.

[9] Mani T, Mahinpey N, Murugan P. Reaction kinetics and mass transfer studies of biomass char gasification with CO_2. Chemical Engineering Science. 2011;66(1):36-41.

[10] Mitsuoka K, Hayashi S, Amano H, Kayahara K, Sasaoaka E, Uddin MA. Gasification of woody biomass char with CO_2: The catalytic effects of K and Ca species on char gasification reactivity. Fuel Processing Technology. 2011;92(1):26-31.

[11] Irfan MF, Arami-Niya A, Chakrabarti MH, Wan Daud WMA, Usman MR. Kinetics of gasification of coal, biomass and their blends in air (N_2/O_2) and different oxy-fuel (O_2/CO_2) atmospheres. Energy. 2012;37(1):665-72.

[12] Lahijani P, Zainal ZA, Mohamed AR. Catalytic effect of iron species on CO_2 gasification reactivity of oil palm shell char. Thermochimica Acta. 2012;546(0):24-31.

[13] Umeki K, Moilanen A, Gómez-Barea A, Konttinen J. A model of biomass char gasification describing the change in catalytic activity of ash. Chemical Engineering Journal. 2012;207–208(0):616-24.

[14] Aho A, DeMartini N, Pranovich A, Krogell J, Kumar N, Eränen K, et al. Pyrolysis of pine and gasification of pine chars – Influence of organically bound metals. Bioresource Technology. 2013;128(0):22-9.

[15] Wall TF, Liu G-s, Wu H-w, Roberts DG, Benfell KE, Gupta S, et al. The effects of pressure on coal reactions during pulverised coal combustion and gasification. Progress in energy and combustion science. 2002;28(5):405-33.

[16] Roberts DG, Harris DJ, Wall TF. On the Effects of High Pressure and Heating Rate during Coal Pyrolysis on Char Gasification Reactivity. Energy & Fuels. 2003;17(4):887-95.

[17] Roberts DG, Hodge EM, Harris DJ, Stubington JF. Kinetics of Char Gasification with CO_2 under Regime II Conditions: Effects of Temperature, Reactant, and Total Pressure. Energy & Fuels. 2010;24(10):5300-8.

[18] Roberts DG, Harris DJ. High-Pressure Char Gasification Kinetics: CO Inhibition of the C–CO2 Reaction. Energy & Fuels. 2012/01/19 2011;26(1):176-84.

[19] Fermoso J, Stevanov C, Moghtaderi B, Arias B, Pevida C, Plaza MG, et al. High-pressure gasification reactivity of biomass chars produced at different temperatures. Journal of Analytical and Applied Pyrolysis. 2009;85(1–2):287-93.

[20] Cetin E, Moghtaderi B, Gupta R, Wall TF. Influence of pyrolysis conditions on the structure and gasification reactivity of biomass chars. Fuel. 2004;83(16):2139-50.

[21] Cetin E, Moghtaderi B, Gupta R, Wall TF. Biomass Gasification Kinetics: Influences of Pressure and Char Structure. Combustion Science and Technology. 2005;177(4):765 - 91.

[22] Illerup JB, Rathmann O. CO2 gasification of wheat straw, barley straw, willow and giganteus. Fuel and Energy Abstracts. 1997;38(1):36-.

[23] Blackwood J, Ingeme A. The Reaction of Carbon with Carbon Dioxide at High Pressure. Australian Journal of Chemistry. 1960;13(2):194-209.

[24] Bhat A, Ram Bheemarasetti JV, Rajeswara Rao T. Kinetics of rice husk char gasification. Energy Conversion and Management. 2001;42(18):2061-9.

[25] Ollero P, Serrera A, Arjona R, Alcantarilla S. The CO_2 gasification kinetics of olive residue. Biomass and Bioenergy. 2003;24(2):151-61.

[26] Barrio M, Hustad JE. CO_2 Gasification of Birch Char and the Effect of CO Inhibition on the Calculation of Chemical Kinetics. Progress in Thermochemical Biomass Conversion: Blackwell Science Ltd; 2008:47-60.

[27] Tancredi N, Cordero T, Mirasol JR, Rodriguez JJ. CO_2 gasification of eucalyptus wood. Fuel. May 20, 1996 1996;75(13):4.

[28] DeGroot WF, Shafizadeh F. Kinetics of gasification of Douglas Fir and Cottonwood chars by carbon dioxide. Fuel. 1984;63(2):210-6.

[29] Molina A, Mondragón F. Reactivity of coal gasification with steam and CO_2. Fuel. 1998;77(15):1831-9.

[30] Simons G. Role of Pore Structure in Coal Pyrolysis and Gasification. Progress in energy and combustion science. 1983;9(4):269-90.

[31] Sane A, Zheng Y, Gore JP. A Study of Steam Gasification of Coal with CO2 Control using H2. 6th U.S. National Combustion Meeting. 2009.

[32] Srinivas B, Amundson NR. A single-particle char gasification model. AIChE Journal. 1980;26(3):487-96.

[33] Bhatia SK, Perlmutter DD. A random pore model for fluid-solid reactions: I. Isothermal, kinetic control. AIChE Journal. 1980;26(3):379-86.